



# Exploring oxygen dynamics and depletion in an intensive bivalve production area in the coastal sea off Rushan Bay, China

Wentao Wu<sup>1,2,3</sup>, Jun Liu<sup>1,2</sup>, Alexander F. Bouwman<sup>3,4,5</sup>, Junjie Wang<sup>3,4</sup>,  
Xunqiang Yin<sup>1</sup>, Jiaye Zang<sup>1</sup>, Xiangbin Ran<sup>1,2,\*</sup>

<sup>1</sup>First Institute of Oceanography, Ministry of Natural Resources, Qingdao 266061, PR China

<sup>2</sup>Laboratory for Marine Geology, Qingdao National Laboratory for Marine Science and Technology, Qingdao 266237, PR China

<sup>3</sup>Key Laboratory of Marine Chemistry Theory and Technology, Ministry of Education, Ocean University of China, Qingdao 266100, PR China

<sup>4</sup>Department of Earth Sciences, Faculty of Geosciences, Utrecht University, Princetonlaan 8a, 3584 CB Utrecht, The Netherlands

<sup>5</sup>PBL Netherlands Environmental Assessment Agency, Postbus 30314, 2500 GH The Hague, The Netherlands

**ABSTRACT:** Hypoxia is a mounting problem affecting the world's coastal waters, with severe consequences for marine ecosystems. Coastal oxygen consumption has been increasing, mainly owing to the continued spread nutrient discharges. Using field observations, incubation experiments and numerical modeling, we studied the spatial and temporal variability of dissolved oxygen (DO) in the coastal area off Rushan Bay, China, a typical coastal area influenced by intensive mariculture oyster production. Results show that summer DO is increasingly declining in bottom waters below the thermocline. Oxygen input from the air–sea interface exchange, primary production and net water exchange accounted for 70, 26 and 4 % of the DO supply, respectively. Oxygen consumption by organic matter decomposition in the water column and sediment contributed, respectively, 79 and 21 % to the total DO removal. In regions such as the coastal area off Rushan Bay where the algal biomass filtered by bivalves is imported from elsewhere by sea currents, the carbon and nutrient release by mariculture may lead to local oxygen depletion, which increased from a negligible contribution in 1984 to up to 24 % of the total DO consumption in the water column in the period of June–September 2014. This phenomenon of oxygen depletion is a concern for other coastal areas with intensive bivalve and other shellfish production.

**KEY WORDS:** Dissolved oxygen · Hypoxia · Sediment · Water column · Oxygen budget · Rushan Bay · Mariculture

*Resale or republication not permitted without written consent of the publisher*

## 1. INTRODUCTION

Hypoxia develops when oxygen demand in bottom waters driven by organic matter decay outpaces replenishment from the oxygen-rich surface (Diaz & Rosenberg 2008, Bianchi et al. 2010, Breitburg et al. 2018). Oxygen demand increases when organic matter production increases as a result of eutrophication (Breitburg et al. 2018). Over the past decades, hypoxic zones (areas with O<sub>2</sub> concentrations <2 mg

l<sup>-1</sup>) in the global coastal ocean have spread rapidly (Diaz & Rosenberg 2008), especially in estuaries and coastal seas that directly receive nutrient inputs from rivers (Breitburg et al. 2018). At present, declining oxygen in coastal waters is one of the most important global environmental problems (Breitburg et al. 2018).

Biogeochemical processes in coastal marine ecosystems often respond in a non-linear fashion to hypoxia (Zhang et al. 2010) or low-oxygen conditions (O<sub>2</sub> con-

\*Corresponding author: rxb@fio.org.cn

centrations  $<4 \text{ mg l}^{-1}$ ) (Karim et al. 2002, Paerl et al. 2006, Liu et al. 2016). Hypoxia seriously impacts coastal marine ecosystems. The reducing environment created under low-oxygen conditions affects carbon, nitrogen, phosphorus, iron, manganese and sulfur chemistry (Middelburg & Levin 2009, Liu et al. 2016, 2020), and results in the accumulation of toxic substances and reactivation and release of harmful chemicals into the water column (Riedel et al. 1999). Ultimately, hypoxia leads to die-off of fish populations and benthic fauna (Vaquer-Sunyer & Duarte 2008, Breitbart et al. 2018), and damage to mariculture production (Liu et al. 2012, 2016). Furthermore, anoxia/hypoxia may contribute to climate change by facilitating methanogenesis and denitrification, which cause enhanced emissions of greenhouse gases (e.g. methane and nitrous oxide) (Egger et al. 2016).

In 2018, China's total mariculture production reached 20.3 Mt, with a major share (71%) for shellfish (Fisheries Bureau of Ministry of Agriculture of the People's Republic of China 2019). The coastal zones of the Yellow Sea account for 25% of China's oyster production (Fisheries Bureau of Ministry of Agriculture of the People's Republic of China 2019). Intensive mariculture may contribute to local low-oxygen conditions. Shellfish filter seston from the water column, excrete organic waste and dissolved nutrients (Shumway et al. 2003, Bouwman et al. 2013a) and consume oxygen (Casas et al. 2018). The nutrients released by shellfish stimulate algal growth, and decay of algal biomass and excreted feces may thus contribute to oxygen depletion (Bouwman et al. 2013b, Casas et al. 2018). With increasing nutrient inputs from mariculture, rivers and atmospheric deposition, the concentration of dissolved oxygen (DO) in the Yellow Sea shows a declining trend over the past decades (Lin et al. 2005, Li et al. 2015).

The high-value oyster production of Rushan City and Haiyang City was worth 4 billion RMB (ca. 586 million US\$) in 2014 (Fisheries Bureau of Ministry of Agriculture of the People's Republic of China 2015). While mariculture rapidly developed in this area from 6300 to 554 000  $\text{t yr}^{-1}$  between 1984 and 2014 (Table S1 in the Supplement at [www.int-res.com/articles/suppl/m649p053\\_supp.pdf](http://www.int-res.com/articles/suppl/m649p053_supp.pdf)), seasonal hypoxia has been reported in Rushan Bay and its coastal area in recent years (Ran et al. 2011), causing increasing economic losses as a result of massive death of cultured shellfish since the 1990s (Ma et al. 1996, Xin et al. 1997, Wang et al. 2012, He et al. 2015). This problem could become worse with expanding mariculture in the coming years.

Many hypoxia studies have been conducted in China's estuarine areas, focusing on organic matter and nutrient inputs from large rivers (Li et al. 2002, Wang 2009, He et al. 2014). However, studies are lacking on hypoxia in nearshore zones like Rushan Bay, with intensive mariculture production but no carbon and nutrient inputs from large rivers. We explored the key factors driving the distribution, production and consumption of DO in the water column and sediment, and the occurrence of oxygen depletion in the coastal areas off Rushan Bay; we used hydrological and sediment data collected in 2009, 2014 and 2016, and applied the results from incubation experiments and modeling to construct an oxygen budget for the study area. The present study aims to improve the understanding of the biogeochemical process of DO in the coastal area affected by shellfish mariculture and to provide a scientific basis for regional environmental protection.

## 2. MATERIALS AND METHODS

### 2.1. Study area

The coastal area off Rushan Bay, China, is located in the south of Shandong Peninsula (Fig. 1), with depths ranging from 5 to 30 m and averaging  $\sim 20 \text{ m}$ . The Rushan River is the major source of sediments entering Rushan Bay, contributing  $0.3\text{--}0.4 \text{ Mt yr}^{-1}$ . The river discharge is approximately  $0.25 \text{ km}^3 \text{ yr}^{-1}$  (0.5% of the water volume in this study area) (Com-

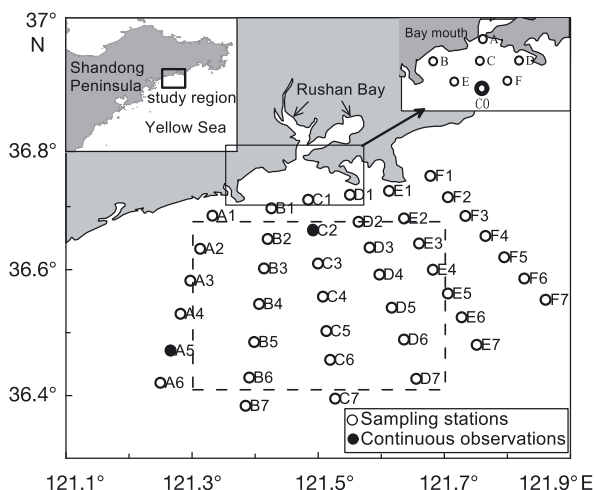


Fig. 1. Sampling stations along 6 transects (labeled A–F) in the coastal area off Rushan Bay, China. The dashed line delineates the area for the dissolved oxygen budget calculation (ranging from 121.4 to 121.7°E and from 36.4 to 36.7°N)

mittee for the Compilation of the Geography of Chinese Coasts 1993). The shallow coastal area is predominantly influenced by the regular semidiurnal tidal current, while the Yellow Sea Cold Water Mass located in the central Yellow Sea with depths >50 m can also extend to the edge of our study area in summer. The study area is also influenced by the Yellow Sea Coastal Current, which flows in the north of the southern Yellow Sea in a southeastward direction along the southern Shandong Peninsula.

The study area is not eutrophic or hypoxic based on its nutrient condition and oxygen level (Ran et al. 2011). However, it is increasingly impacted by mariculture (especially shellfish culture in mudflats) and urban and industrial effluents in recent decades (Table S1).

## 2.2. Sampling and analytical methods

Three types of investigation were carried out in the coastal area off Rushan Bay: (1) monthly observations of hydrological, chemical and biological parameters at 47 sampling stations along 6 transects (A–F; Fig. 1) during June–September 2009; (2) continuous observations at Stns A5 and C2 for 24 h (22 August 2009) to determine the influence of tidal currents; and (3) supplementary surveys of primary production and oxygen consumption in water and sediment at Stns C1, C2 and C5 in August 2014 and at C2 in August 2016.

Water samples were collected at depths of 0.5, 5 and 10 m and in the bottom water (<2 m above the sea floor) using water samplers attached to a CTD system (JFE, AAQ122), and hydrological parameters (e.g. water temperature and salinity) were obtained simultaneously. About 150 ml of water were transferred immediately to flasks using a siphon, and DO concentration was measured via Winkler titration using a Coulomb Titrator (Metrohm, 877 Titrino plus) after addition of  $\text{MnCl}_2$  and alkaline KI reagent, with a relative standard deviation (RSD) <0.3%. About 1 l of water was filtered with a 0.45  $\mu\text{m}$  cellulose acetate membrane (pre-cleaned with 1:1000 HCl for 24 h and then washed with Milli-Q water to neutral pH, oven-dried at 45°C) and the filtrate was stored in the dark at –20°C for determination of nitrate ( $\text{NO}_3\text{-N}$ ), nitrite ( $\text{NO}_2\text{-N}$ ), ammonium ( $\text{NH}_4\text{-N}$ ), active phosphate ( $\text{PO}_4\text{-P}$ ) and silicate ( $\text{SiO}_3\text{-Si}$ ) using a nutrient auto-analyzer (SEAL Analytical, QuAAtro). The filters were stored in the dark to analyze chlorophyll *a* (chl *a*) using a fluorescence spectrophotometer (Electrical Instrument, 970 CRT) after extraction with 9:1

(v/v) acetone. Finally, the remaining unfiltered water samples were stored at 4°C in the dark for determination of chemical oxygen demand (COD), total phosphorus (TP) and total nitrogen (TN). COD was analyzed according to standard methods in the Chinese national specifications for marine monitoring (National Marine Environmental Monitoring Center 2007). Briefly, under alkaline heating conditions, excess potassium permanganate was used to oxidize the aerobic substances in seawater; under acidic sulfuric acid conditions, excess potassium permanganate and manganese dioxide were then reduced with potassium iodide and the generated free iodine was titrated with sodium thiosulfate standard solution. TN and TP were also determined by the auto-analyzer using the method described by Grasshoff et al. (1999). The RSDs for nutrient measurements were 5–10% (Ran et al. 2011). Statistical analyses were conducted using SPSS 18.0 software. Surfer 11.0 and Origin 8.5 were used for mapping the concentration patterns. A 2-sample *t*-test was used to explore differences in our observations at a significance level of 0.05.

## 2.3. Calculation of the DO budget

The DO budget was calculated for the coastal area off Rushan Bay (Fig. 1). The oxygen input in the budget includes the net DO flux from water exchange ( $F_{\text{in}}$  minus  $F_{\text{out}}$ ) (see Section 2.3.1), air–sea exchange ( $F_{\text{A-S}}$ ) (Section 2.3.2) and primary production ( $F_{\text{pp}}$ ) (Section 2.3.3). DO output includes consumption in the water column ( $F_{\text{oc(water)}}$ ), which includes the contribution  $F_{\text{ma}}$  by mariculture through the release of dissolved carbon and nutrients (Section 2.3.4) and in sediments ( $F_{\text{oc(sediment)}}$ ) (Section 2.3.5).

### 2.3.1. Water inflow and outflow

The variable grid zero-dimensional steady-state Princeton Ocean Model (POM) (Sun et al. 2014) (Fig. 2) was used to calculate oxygen exchange in water inflow ( $F_{\text{in}}$ ) and outflow ( $F_{\text{out}}$ ). The hydrography in the coastal area off Rushan Bay is dominated by semidiurnal tidal currents. Local tide, tidal currents (K1, O1, M2 and S2, see Figs. S1–S4), flow rate and direction were simulated by POM. Tide and flow rates were combined with the water depth and DO measurements to calculate the contribution of horizontal transport to the DO budget of the coastal area off Rushan Bay (Fig. 2).

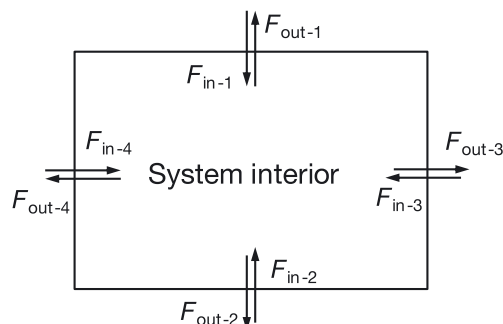


Fig. 2. Scheme of dissolved oxygen (DO) fluxes across the boundaries of the coastal area off Rushan Bay shown in Fig. 1

### 2.3.2. Air–sea oxygen exchange ( $F_{A-S}$ )

The DO exchange flux at the air–sea interface was calculated using the following equation (Skjelvan et al. 2001):

$$F_{A-S} = -k_1 ([O_2]_m - [O_2]_s) \quad (1)$$

where  $F_{A-S}$  is the flux of oxygen at the air–sea interface over the coastal area off Rushan Bay ( $\text{mg m}^{-2} \text{d}^{-1}$ );  $[O_2]_m$  is the measured oxygen concentration in the surface water ( $\text{mg l}^{-1}$ ) and  $[O_2]_s$  is the corresponding saturation concentration (Weiss 1970);  $k_1$  is the gas transfer velocity ( $\text{m d}^{-1}$ ), calculated according to Wanninkhof (1992) (for details see Section S1 in the Supplement); study area ( $\text{m}^2$ ) and time (d) were used to estimate the total inflow/outflow (units in Gg) of oxygen off Rushan Bay. Positive values of  $F_{A-S}$  indicate fluxes to the water, while negative values indicate fluxes to the atmosphere.

### 2.3.3. Oxygen production by primary production ( $F_{PP}$ )

The rates of primary production were determined at Stns C1, C2 and C5 by incubation of CTD-collected samples in both light (respiration + photosynthesis) and dark (respiration; wrapped in aluminum foil to prevent photosynthesis) bottles (250 ml) (Falkowski & Raven 1997, Fahey & Knapp 2007). The light and dark bottles were placed back at the original sampling depth for 8 h incubation (from 08:00 to 16:00 h) and then removed for immediate DO measurement. Secchi depth was measured using a Secchi panel on board.

Oxygen production during photosynthesis was calculated based on the changes in oxygen inside the light and dark bottles, chl *a* concentration and incu-

bation time (Behrenfeld & Falkowski 1997), and integrated with the euphotic depth (for details see Section S2 in the Supplement).

### 2.3.4. Oxygen consumption in the water column ( $F_{oc(\text{water})}$ )

DO consumption rates by microbial respiration in the water column ( $F_{oc(\text{water})}$ ) were measured at Stns C1, C2 and C5 by monitoring temporal changes in oxygen concentration of unfiltered water incubated in 250 ml BOD bottles in dark (wrapped in aluminum foil to prevent photosynthesis) at the original sampling depth. Control treatments (where biological respiration was inhibited) were included with 0.1% (v/v) saturated  $\text{HgCl}_2$  added at the initial time of the experiment (He et al. 2014). The oxygen consumption rates were calculated from the DO decrease during incubation.

Nitrification rates were also measured with the incubation approach at Stns C1, C2 and C5 (Bierman et al. 1994, He et al. 2014). Three sets of experiments were set up for each station, and water samples were dispensed into 1 l narrow-neck brown glass bottles. Allylthiourea ( $\text{C}_4\text{H}_8\text{N}_2\text{S}$ ;  $100 \text{ mg l}^{-1}$ ) was added into 1 incubation bottle to inhibit the oxidation of ammonia to nitrite,  $\text{NaClO}_3$  ( $10 \text{ mg l}^{-1}$ ) was simultaneously added into another incubation bottle to inhibit the oxidation of nitrite to nitrate, and the third incubation bottle was the control without an inhibitor. After incubation for 0, 2, 6, 12, 18 and 24 h, 20 ml were extracted from each bottle and filtrated. The filtrate was dispensed into polyethylene containers (acidified with 1:5 HCl for 48 h and rinsed with Milli-Q water several times) and stored at  $-20^\circ\text{C}$  for the determination of dissolved nitrogen. Nitrification rates were estimated from the production of nitrite during incubation in the 3 sets of bottles.

Since nitrification and decomposition of organic matter are the primary biogeochemical processes responsible for DO consumption, we estimated how mariculture enhanced these processes ( $F_{ma}$ ). A nutrient budget model for mariculture (Bouwman et al. 2011) was used to estimate oxygen dynamics through nutrient flows (for details see Section S3 and Fig. S5 in the Supplement) based on long-term (1984–2014) data for mariculture production from various local sources (The People’s Government of Rushan 1985–2015, Yantai Municipal Bureau of Statistics 1985–2015, Shandong Provincial Bureau of Statistics 1990–2008, Weihai Municipal Bureau of Statistics 1990–2015, Shandong Provincial Department of

Oceans and Fisheries 2003–2015) (Table S1). We adopted a dissolved C:N ratio of 21 in the excreta (Fig. S5) according to the carbon and nutrient flows in an oyster reef system (Dame et al. 1989). We assumed that the oxygen consumption rate is 1:1 ( $O_2:C$  in molar ratio) for dissolved C oxidation and 2:1 ( $O_2:N$  in molar ratio) for nitrate nitrification, respectively (Bierman et al. 1994, He et al. 2014) to compute total annual oxygen consumption from aquaculture for 1984–2014 (Table S1). It should be noted that  $F_{ma}$ , as a part of oxygen consumption in the water column, includes respiration and nitrification. Since the DO budget was calculated for a 4 mo period in this study, and the modeled DO due to mariculture was modeled yearly during 1984–2014, we used 1/3 of the annual loading to estimate the contribution of mariculture to the water DO consumption in the period of June–September 2014.

### 2.3.5. Oxygen consumption in the sediment

$$(F_{oc(sediment)})$$

Sediment oxygen demand ( $F_{oc(sediment)}$ ) was determined at Stns C1, C2 and C5, where surface sediment was collected with a box corer, and the surface layer (0–2 cm) was scraped off into a sealed ziplock bag after the overlying water was removed. Subsequently, the sample bags were filled with  $N_2$  at 4°C before incubation experiments. Bottom water samples were collected *in situ* and filtered through 0.45  $\mu m$  pore size polyethersulfone filters and injected into the headspace above the sediments at a modulated speed to avoid visible sediment re-suspension. The sediment, in tightly sealed bags with any remaining air removed, was held at 20°C (the average temperature of bottom water in August) in the dark for *in situ* incubation experiments. DO concentration of the incubation water was determined at the start and end of the incubation. The oxygen consumption rate in sediments was obtained from Liu et al. (2016):

$$SOD = (C_t - C_0) \times V / (t \times S) \quad (2)$$

where SOD is the sediment oxygen demand ( $mg\ m^{-2}\ d^{-1}$ ),  $C_0$  and  $C_t$  represent the initial and post incubation DO concentrations ( $mg\ l^{-1}$ ) in the overlying seawater, respectively,  $V$  is the water volume (l),  $t$  is the incubation time (d), and  $S$  is the surface area of the sediment used for the incubation experiment ( $m^2$ ). This approach is based on the benthic diffusive fluxes and the assumption that the contribution of SOD from sediments is mainly induced by the top

sediments, which is reasonable because the oxygen penetration depth is fairly small in sediments and this approach has a minor influence of reoxidation from deeper layers.

## 3. RESULTS

### 3.1. General characteristics

The observed temperature, salinity, COD, TN, TP, chl *a* and DO in the coastal area off Rushan Bay during June–September 2009 are listed in Table S2. The seawater temperature was lowest in June and showed no significant variation in the other months. The surface seawater temperature exceeded that in the bottom layer, indicating stratification. Salinity was similar in surface and bottom layers and stable during June–September. Both TN and TP concentrations showed spatiotemporal variations with higher concentrations in June and September than in July and August, and significantly ( $p < 0.05$ ) higher concentrations in the bottom than in the surface in September. The values of COD and chl *a* in July, August and September were higher than those in June (Table S2).

### 3.2. Distribution of DO

DO concentrations were higher in June and July than in August and September in the coastal area off Rushan Bay (Table 1). There was a significant difference between the surface and bottom layers ( $p < 0.01$ ). DO concentrations in the surface water were higher and much less variable than those in the bottom layer. The lowest DO concentration in the bottom layer was observed in August.

Throughout the study area, the DO concentration of the bottom water was higher in June and July than in August and September. In June, bottom DO concentration in the nearshore water was higher than in the offshore water, fairly high in the northwest and decreasing in the east–west direction in July. The distribution of DO in the bottom water in August was similar to that in June, with higher concentrations in offshore than in nearshore areas. In September, the DO concentration of bottom water was low in the middle of the offshore area (Fig. 3).

The bottom water oxygen solubility was lower in June and July than in August and September (Fig. S6). In June, the oxygen solubility was higher in the middle of the southeast direction and lower in

Table 1. Dissolved oxygen concentrations ( $\text{mg l}^{-1}$ ) in the coastal area off Rushan Bay in June, July, August and September 2009. Means are given  $\pm$ SD

Level	Range	Mean	n
<b>June</b>			
Surface	6.79–8.14	$7.50 \pm 0.31$	47
5 m	6.76–7.87	$7.42 \pm 0.3$	21
10 m	7.16–8.22	$7.78 \pm 0.26$	15
Bottom	6.00–9.45	$7.44 \pm 0.73$	47
Whole column	6.00–9.45	$7.47 \pm 0.56$	130
<b>July</b>			
Surface	6.44–11.8	$8.59 \pm 1.58$	47
5 m	6.83–8.53	$7.59 \pm 0.54$	12
10 m	6.76–10.2	$7.87 \pm 0.89$	11
Bottom	4.86–8.56	$6.87 \pm 0.90$	47
Whole column	4.86–11.8	$7.68 \pm 1.82$	117
<b>August</b>			
Surface	5.12–7.26	$6.54 \pm 0.46$	47
5 m	5.12–7.49	$6.69 \pm 0.50$	39
10 m	5.76–7.66	$6.79 \pm 0.45$	26
Bottom	3.21–7.16	$5.10 \pm 0.84$	47
Whole column	3.21–7.66	$6.06 \pm 0.93$	159
<b>September</b>			
Surface	5.92–7.17	$6.64 \pm 0.31$	47
5 m	5.80–7.19	$6.65 \pm 0.39$	19
10 m	5.59–7.14	$6.68 \pm 0.49$	13
Bottom	4.45–6.96	$6.17 \pm 0.52$	47
Whole column	4.45–7.19	$6.41 \pm 0.49$	126

nearshore areas. In July, high oxygen solubility values appeared in the northeast and decreasing southwestward. In August, similar to June, there were high values in the offshore and lowest values (35%) in the southwest direction. In September, lower values appeared in the southern direction.

The DO concentrations in surface water at Stns C2 and A5 were  $6.91$  ( $6.71$ – $7.71$ ) and  $7.23$  ( $6.71$ – $7.99$ )  $\text{mg l}^{-1}$ , respectively. Bottom water DO concentrations of  $5.61$  ( $3.76$ – $6.99$ )  $\text{mg l}^{-1}$  at Stn C2 and  $5.83$  ( $3.74$ – $8.26$ )  $\text{mg l}^{-1}$  at Stn A5 were lower than those in surface water. The DO concentrations in surface water showed no clear variation with the tidal range, while that in the bottom layer tended to be lower at high tide and higher at low tide (Fig. 4).

### 3.3. Dissolved oxygen budget

The DO exchange fluxes for the coastal area off Rushan Bay, calculated from the water exchange flux and DO concentrations in the 4 directions (Table 2), indicate a total DO input of 290 Gg and a total output of 260 Gg, which implies a net DO input of 30 Gg for the period June–September.

The air–sea DO exchange ( $F_{A-S}$ ) ranged from  $-1420$  to  $3780$   $\text{mg m}^{-2} \text{d}^{-1}$ , with an average value (mean  $\pm$  SD) of  $1890 \pm 982$   $\text{mg m}^{-2} \text{d}^{-1}$ .  $F_{PP}$  was determined from the DO concentration in light ( $7.29$ – $8.90$   $\text{mg l}^{-1}$ ) and dark bottles ( $6.59$ – $7.71$   $\text{mg l}^{-1}$ ), the chl *a* concentration ( $1.0$ – $2.79$   $\mu\text{g l}^{-1}$ ) and the assimilation coefficient ( $0.86$ – $85.2$   $\text{mg C mg}^{-1} \text{chl } a \text{ h}^{-1}$ ). The calculated oxygen production during photosynthesis was therefore between  $96.5$  and  $1140$   $\text{mg m}^{-2} \text{d}^{-1}$ , with an average value of  $552$   $\text{mg m}^{-2} \text{d}^{-1}$ .

The oxygen consumption rate by microbial respiration in the water column was  $102$   $\text{mg m}^{-3} \text{d}^{-1}$  ( $56$ – $220$ ). The nitrification rate was  $1.6$   $\text{mg m}^{-3} \text{d}^{-1}$  ( $0.96$ – $2.4$ ), and accounted for 1.5% of the total oxygen consumption (microbial respiration and nitrification) in the water column (Fig. 5), while oxygen consumption by microbial respiration and decomposition made up >98%. Total oxygen consumption in the water column exceeded that in the sediment by a factor of 2.8.

The sediment oxygen consumption caused an exponential decline of DO during the incubation process (Fig. 6). This DO consumption is approximately linear during the initial 10 h, and this amount is equivalent to  $560$   $\text{mg m}^{-2} \text{d}^{-1}$ .

The resulting DO budget based on our 2009 and 2014 observations shows that the total amount of DO produced by primary production was about 230 Gg during June–September, and the  $F_{A-S}$  was 620 Gg. Oxygen consumption by sediments was 180 Gg, and the total oxygen consumption in the water column was 680 Gg. The net flux of DO (inflow minus outflow) was 30 Gg (Fig. 7).

The estimated nitrogen release from bivalve mariculture in the study area was  $4.5$   $\text{Gg yr}^{-1}$  in 2014 (Table S1), and the release of dissolved C was  $95$   $\text{Gg yr}^{-1}$ . This yields an oxygen consumption of  $253$   $\text{Gg yr}^{-1}$  for 2014 (Table S1). Oxygen consumption by nitrification of the ammonia released by shellfish adds another  $21$   $\text{Gg yr}^{-1}$ , which yields a total oxygen consumption of  $274$   $\text{Gg yr}^{-1}$  for 2014 (Fig. 8). Using the high C:N ratio to compute dissolved C release from the shellfish results in a total oxygen consumption of  $483$   $\text{Gg}$  in 2014 (Table S1), which is almost one-quarter of the total DO consumption in the water column (Fig. 7).

## 4. DISCUSSION

The chl *a* levels were generally low (except the extremes in July), and DO levels never reached sub-oxic levels except in early August in the coastal area off Rushan Bay (Tables 1 & S2, Fig. S6). Although the

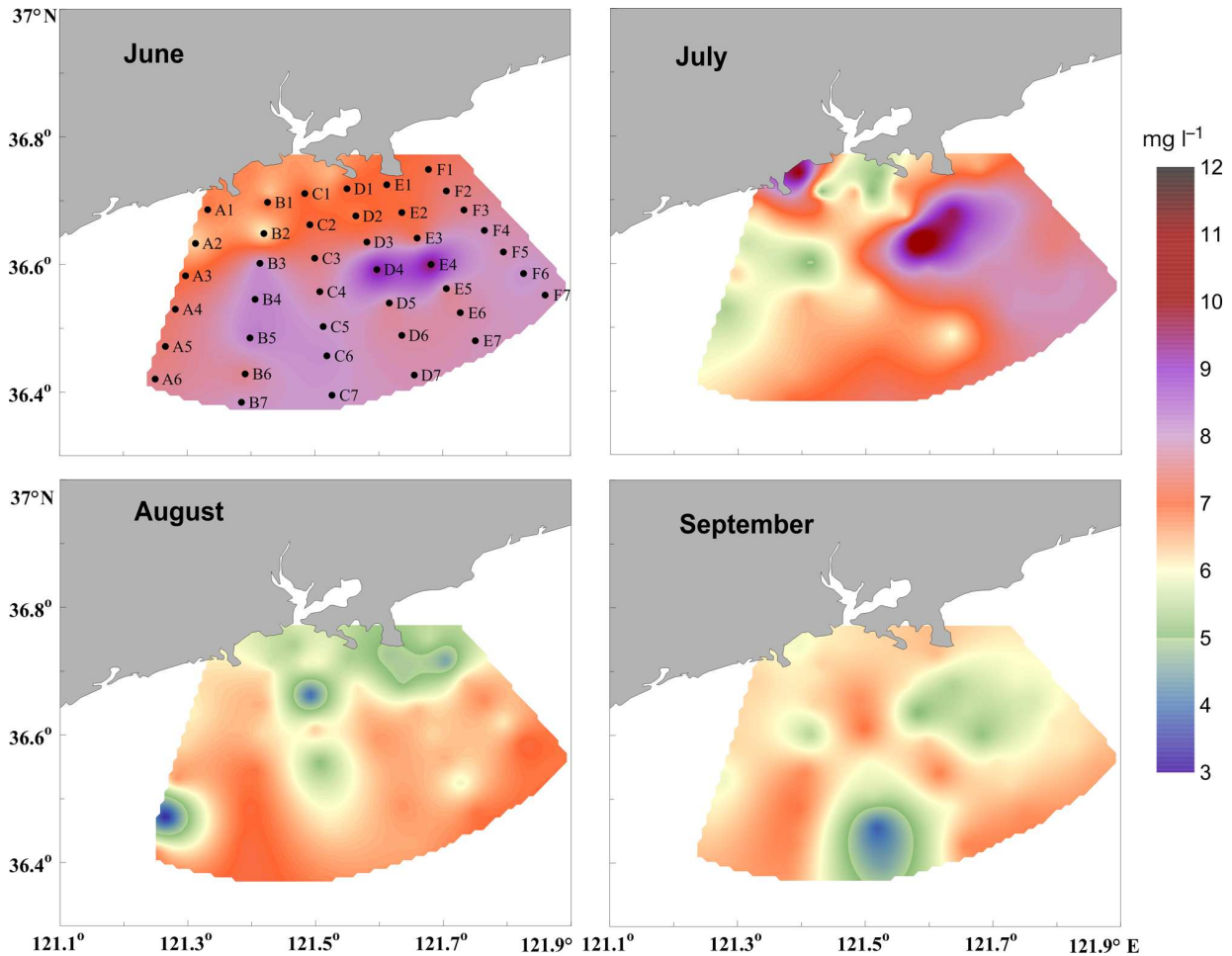
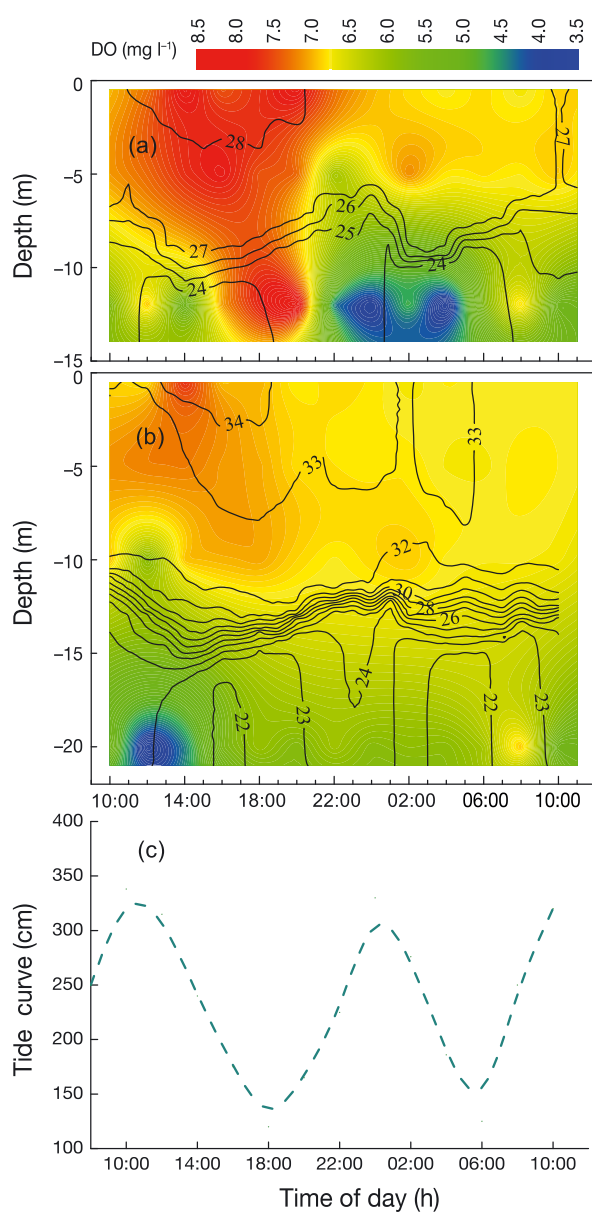


Fig. 3. Horizontal distribution of bottom water dissolved oxygen (DO) concentration in the coastal area off Rushan Bay in June, July, August and September 2009

coastal area off Rushan Bay is not yet eutrophic or hypoxic according to its nutrient and DO concentrations, abrupt changes in nutrient and organic states have occurred in both Rushan Bay and the coastal area off Rushan Bay under increasingly intense anthropogenic activities (Ma et al. 1996, Xin et al. 2004, Zang et al. 2017). The observed DO contents in the bottom water off Rushan Bay in this study are lower than those observed in the shelf area around the Yellow Sea (Wang et al. 1999). The sediment oxygen consumption rate of  $560 \text{ mg m}^{-2} \text{ d}^{-1}$  measured in this study is similar to that measured in Jiaozhou Bay and Sanggou Bay ( $330 \text{ mg m}^{-2} \text{ d}^{-1}$ ) (Zhang et al. 2006) and much higher than in the Yellow Sea ( $61 \text{ mg m}^{-2} \text{ d}^{-1}$ ), East China Sea ( $134 \text{ mg m}^{-2} \text{ d}^{-1}$ ) (Song et al. 2016) and Baltic Sea ( $174 \text{ mg m}^{-2} \text{ d}^{-1}$ ) (Almroth et al. 2009). The abundance of organic carbon could be a

key factor in the difference of oxygen consumption rates, and the organic carbon contents in sediments are much higher in the coastal zone off Rushan Bay than those in the Yellow Sea and the East China Sea (Song et al. 2016).

The coastal area off Rushan Bay experiences low-oxygen conditions in summer (Ran et al. 2011), a phenomenon which is becoming more prominent as the COD increases: from  $0.59 \text{ mg l}^{-1}$  in the 1990s (Ma et al. 1996) to  $0.71\text{--}1.77 \text{ mg l}^{-1}$  at present. Compared with historical data for the coastal area off Rushan Bay (Ma et al. 1996, Xin et al. 2004), we observed an increase in COD and decreasing DO values. Similar oxygen depletion also occurred in other sea regions such as the Laizhou Bay, Beibu Gulf, southern Yellow Sea and the central Bohai Sea (Cui et al. 1994, Zu et al. 2005, Zhai et al. 2012).



In the following sections, we first discuss the spatial distribution of DO and its monthly variation under the influence of DO production and consumption and that of the hydrodynamics on mixing of DO-rich surface water and DO-depleted bottom water (Section 4.1). The DO budget of the study area, contribution of mariculture to DO depletion and their changes are further discussed in Sections 4.2 and 4.3.

#### 4.1. Monthly variation in the spatial distribution of DO

Our observations during June–September show that both the largest low-oxygen area and lowest DO concentrations occur in August. DO concentrations of bottom waters in coastal areas are generally related to stratification, which hinders vertical replenishment of oxygen from the oxygen-rich surface water, in combination with oxygen consumption processes (Long et al. 2019). Since the stratification is most pronounced in August, the extent and area of low-oxygen conditions is also largest in August. The observed DO concentration in the coastal area off Rushan Bay was higher nearshore than offshore (Fig. 3) and higher in surface water with less spatial variation than in the bottom water (Table 2). There was a distinct thermocline in June–September (Fig. 4), which reduced the DO exchange between the oxygen-rich surface and oxygen-poor bottom waters. This is confirmed by our 24 h continuous observations, which showed that all low-oxygen regions were below the thermocline (Fig. 4). The surface DO concentration was signi-

Fig. 4. Vertical cross sections of dissolved oxygen (DO) concentrations at (a) Stn C2 and (b) Stn A5 and (c) average tide level simulated by the Princeton Ocean Model during 24 h on 22 August 2009; the black contours show isopleths of temperature ( $^{\circ}\text{C}$ )

Table 2. Mean depth, length of the sides and cross-sectional area, water velocity, net water flux exchange through the boundary, dissolved oxygen (DO) concentration and DO flux for the north, south, east and west sides of the coastal area off Rushan Bay, China, for the period June–September ( $F_i$  is the net flux of DO, calculated by the water discharge at boundary  $i$  and its DO concentration;  $i = 1-4$ ). Mean flow velocity is the net flow velocity accounting for reciprocating movement of water, where positive (negative) values represent inflow to (outflow from) the system

Boundaries	Mean depth (m)	Side length (km)	Cross section area ( $\text{km}^2$ )	Mean flow velocity ( $\text{m s}^{-1}$ )	Water exchange flux ( $\text{km}^3 \text{d}^{-1}$ )	Mean DO concentration ( $\text{mg l}^{-1}$ )	DO flux (Gg)
North side ( $F_1$ )	16	54	0.87	0.005	0.19	7.27	129
South side ( $F_2$ )	26	54	1.40	-0.004	-0.24	6.79	-150
East side ( $F_3$ )	23	33	0.77	0.007	0.24	7.36	159
West side ( $F_4$ )	20	33	0.68	-0.007	-0.19	6.79	-107



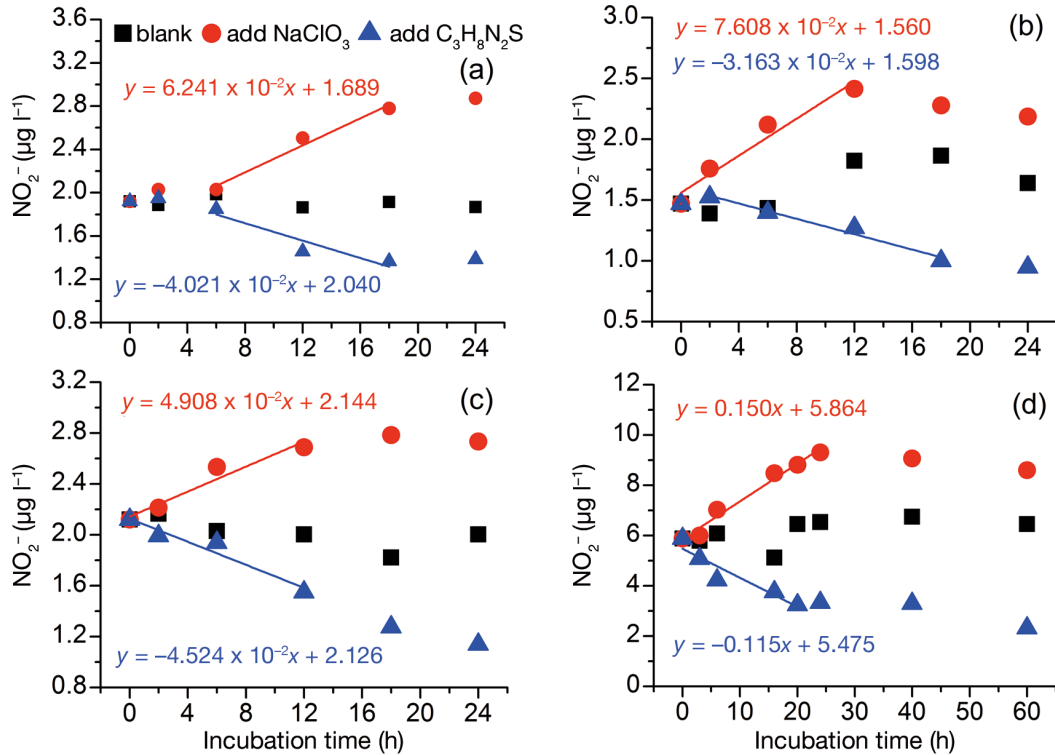


Fig. 5. Nitrite concentration over time for determination of nitrification reactions at (a) Stn C1, (b) Stn C2 and (c) Stn C5 (c) in August 2014 and (d) Stn C2 in August 2016. For details of the experiment, see Section 2.3.4

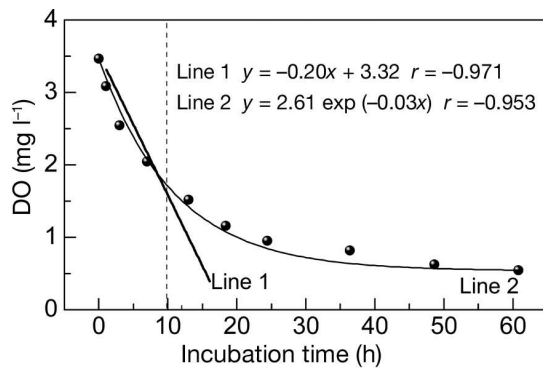


Fig. 6. Dissolved oxygen (DO) concentration determined in the seawater overlying the surface sediment. The vertical dashed line describes the first, linear phase of the oxygen consumption during the incubation process; the regression equation of Line 1 was used to estimate the DO consumption rate during this phase

ificantly higher than that in bottom water in the continuous observations ( $p < 0.05$ ).

DO concentrations are strongly influenced by the tidal range, as the DO concentrations at different depths at Stns C2 and A5 (Fig. 4) indicate that DO concentrations below the thermocline at low tide

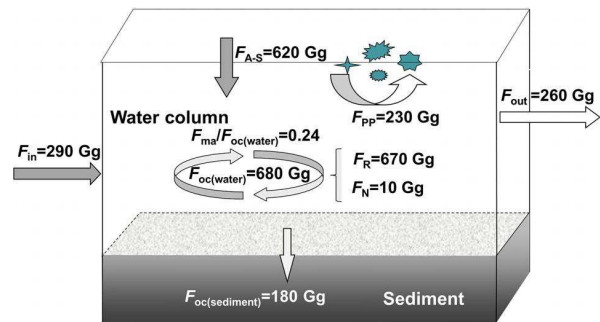


Fig. 7. Dissolved oxygen (DO) budget in the coastal area off Rushan Bay in June–September with the following DO fluxes:  $F_{in}$ : inflow;  $F_{out}$ : outflow;  $F_{PP}$ : supply by primary production;  $F_{A-S}$ : supply by air–sea gas exchange;  $F_{oc(water)}$ : total oxygen consumption in the water column;  $F_{oc(sediment)}$ : consumption in sediment;  $F_{ma}$ : consumption associated with mariculture, which equals to 1/3 of annual loading;  $F_N$ : consumption by nitrification;  $F_R$ : consumption by microbial respiration;  $F_{oc(water)} = F_N + F_R$ . The star-like symbols represent the primary production

exceed those at high tide. Thus, tides have an important impact on the bottom DO concentration in the nearshore, shallow water by vertical mixing. The bottom DO concentration is also affected by temper-

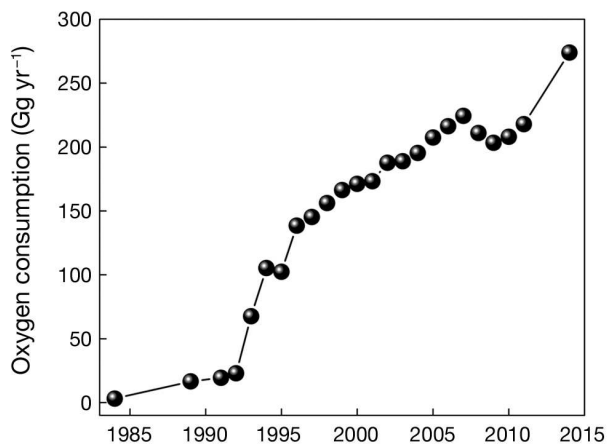


Fig. 8. Oxygen consumption associated with mariculture in the coastal area off Rushan Bay in past decades

ature as illustrated by the negative correlation between DO and temperature in June and September and the positive correlation in July and August (Table S3). This implies that the thermocline in July and August weakened the water and oxygen exchange between surface and bottom water.

Apart from stratification, the occurrence of low-oxygen conditions in summer is also related to enhanced oxygen consumption by decomposition of organic matter produced by algae in the nearshore areas as indicated by the high chl *a* values, particularly when there is stratification (Li et al. 2002, Zhai et al. 2012). DO and chl *a* were positively correlated in June and July. This is largely due to the oxygen produced during phytoplankton growth in July, as indicated by the higher chl *a* contents in the water, causing the highest average DO saturation percentage (123%). DO oversaturation also occurred in some of the bottom water samples (Fig. S6). In August and September, DO consumption occurred due to decaying phytoplankton biomass.

#### 4.2. How mariculture changed the DO budget

Our DO budget (Fig. 7) suggests the importance of hydrodynamics and biogeochemical processes for DO supply and consumption. Most of the DO supply is from air–sea gas exchange (70%) and primary production (26%), while the net inflow into the coastal area off Rushan Bay contributes only 4%. The total DO supply (850 Gg for months between June and September) is consumed mostly in the water column (79%) and the remainder in the sediments (21%). In summer, the total DO consumption exceeds the total

DO supply, which together with stratification leads to low-oxygen conditions in the bottom water off Rushan Bay.

Total mariculture production has increased dramatically over the past decades, with oysters, other bivalves and shellfish accounting for more than 90% (544 Gg yr<sup>-1</sup>) in 2014 (Table S1). Using the aquaculture nutrient budget model presented by Bouwman et al. (2011), we estimated an annual release of 95 Gg dissolved C yr<sup>-1</sup> and oxygen consumption of 253 Gg yr<sup>-1</sup> for 2014 (Table S1) on the basis of a dissolved C:N ratio of 21 in the excreta (Dame et al. 1989). Nitrification of primarily ammonia-N by bivalves consumes another 21 Gg of oxygen. However, as the C:N ratio in the excreta from the mariculture system could be much higher based on the standard error of this ratio (Dame et al. 1989), the contribution of bivalve mariculture to total oxygen consumption in the study area may amount to 24% for the period of June–September in 2014. Our results indicate that the oxygen consumption has been rising steadily since the 1980s (Fig. 8).

Many studies suggest that bivalves filter seston from the water and act as water cleaners in mariculture systems (Shumway et al. 2003, Lindahl 2011). Oyster growth can reduce eutrophication by enhancing denitrification rates and assimilating nutrients into macrofauna (Kellogg et al. 2013). Thus, there would be a net removal of organic matter and nutrients therein (Zang et al. 2017) that are imported by the water flow into the Rushan Bay area. However, bivalves also excrete feces and pseudofeces (i.e. material they cannot digest) and dissolved nutrients. While the feces and dissolved C are decomposed, oxygen is consumed; decay of dead algal biomass also consumes oxygen. The increasing carbon and nutrient release by oyster culture (Fig. 8) in combination with summer stratification (Fig. 4) can contribute to increased localized oxygen depletion.

#### 4.3. Implications of increased aquaculture to coastal declining oxygen

The occurrence of coastal hypoxia has been increasing in China in recent years. Apart from the hypoxic zones in the Yangtze River estuary, many new hypoxic regions have recently been developing in Chinese coastal seas, e.g. the Pearl River Estuary and Beibu Gulf, so a further spreading of hypoxia may be expected in the near future.

The coastal area off Rushan Bay is not very eutrophic, with relatively low levels of chl *a*. Our

long-term model results indicate that the increase in marine aquaculture activities has resulted in increasing oxygen depletion. Intensive marine fish and shellfish aquaculture production takes place in many provinces of China (Wang et al. 2020). Mariculture may therefore contribute to the development of hypoxia in other parts of China's coastal waters, especially when combined with other sources of nutrients and organic pollution (Wang et al. 2020).

## 5. CONCLUSIONS

In contrast to other hypoxic regions in China that are impacted by river nutrient export, such as the Yangtze River estuary (Li et al. 2002, Chen et al. 2007, H. Wang et al. 2016, B. Wang et al. 2017) and Pearl River Estuary (Wei et al. 2009, Zhang et al. 2009), the low-oxygen conditions in the coastal area off Rushan Bay in summer seem to be related to oyster mariculture production. Our research provides a case study for understanding oxygen depletion in an intensive mariculture area and its effects on marine ecosystems.

Although bivalve aquaculture is often regarded as a nutrient sink, in conditions where algal biomass is imported by sea currents from elsewhere, the carbon and nutrients released by filter-feeders may lead to local oxygen depletion. Nitrification and decay of dissolved carbon compounds released by the bivalves are the primary biogeochemical processes responsible, currently for up to one-quarter of water DO consumption in the coastal area off Rushan Bay. Oxygen depletion of bottom water below the thermocline is seasonal, and thanks to the tidal currents, there is no development and expansion of serious hypoxia in Rushan Bay. Research on oxygen and hypoxia is needed in other coastal seas where mariculture production takes place, especially in areas with large inputs of organic pollutants and nutrients from rivers and atmospheric deposition.

*Acknowledgements.* This study was supported by the National Natural Science Foundation of China (Nos. 41776089 and 41806097) and the Basic Scientific Fund for National Public Research Institutes of China (No. 2019JH02). A.F.B. received support from Green Card Talents project no. 841912031 financed by Ocean University of China. We thank Yibin Wang, Aijun Zhang and Houqin Xu for their assistance in the field sampling. We also thank Prof. Patricia Glibert (University of Maryland) for her comments on an earlier version of this paper. We have no competing financial interests.

## LITERATURE CITED

- ✦ Almroth E, Tengberg A, Andersson JH, Pakhomova S, Hall POJ (2009) Effects of resuspension on benthic fluxes of oxygen, nutrients, dissolved inorganic carbon, iron and manganese in the Gulf of Finland, Baltic Sea. *Cont Shelf Res* 29:807–818
- ✦ Behrenfeld MJ, Falkowski PG (1997) Photosynthetic rates derived from satellite-based chlorophyll concentration. *Limnol Oceanogr* 42:1–20
- ✦ Bianchi TS, DiMarco SF, Cowan JH, Hetland RD, Chapman P, Day JW, Allison MA (2010) The science of hypoxia in the Northern Gulf of Mexico: a review. *Sci Total Environ* 408:1471–1484
- ✦ Bierman JVJ, Hinz SC, Zhu WD, Wiseman WJ, Rabalais NN, Turner RE (1994) A preliminary mass balance model of primary productivity and dissolved oxygen in the Mississippi River plume/Inner Gulf shelf region. *Estuaries* 17: 886–899
- ✦ Bouwman AF, Pawłowski M, Liu C, Beusen AHW, Shumway SE, Glibert PM, Overbeek CC (2011) Global hindcasts and future projections of coastal nitrogen and phosphorus loads due to shellfish and seaweed aquaculture. *Rev Fish Sci* 19:331–357
- ✦ Bouwman AF, Beusen AHW, Overbeek CC, Bureau DP, Pawłowski M, Glibert PM (2013a) Hindcasts and future projections of global inland and coastal nitrogen and phosphorus loads due to finfish aquaculture. *Rev Fish Sci* 21:112–156
- ✦ Bouwman AF, Beusen AHW, Glibert PM, Overbeek C and others (2013b) Mariculture: significant and expanding cause of coastal nutrient enrichment. *Environ Res Lett* 8: 044026
- ✦ Breitbart D, Levin LA, Oschlies A, Grégoire M and others (2018) Declining oxygen in the global ocean and coastal waters. *Science* 359:eaam7240
- ✦ Casas SM, Lavaud R, La Peyre MK, Comeau LA, Filgueira R, La Peyre JF (2018) Quantifying salinity and season effects on eastern oyster clearance and oxygen consumption rates. *Mar Biol* 165:1–13
- ✦ Chen CC, Gong GC, Shiah FK (2007) Hypoxia in the East China Sea: one of the largest coastal low-oxygen areas in the world. *Mar Environ Res* 64:399–408
- Committee for the Compilation of the Geography of Chinese Coasts (1993) *China Gulf history. Geography of Chinese Coasts*. China Ocean Press, Beijing (in Chinese)
- Cui Y, Yang QF, Song YL (1994) Distribution of phosphate and dissolved oxygen and their relation in the Bohai Sea in summer. *Mar Environ Sci* 13:31–35 (in Chinese)
- ✦ Dame RF, Spurrier JD, Wolaver TG (1989) Carbon, nitrogen and phosphorus processing by an oyster reef. *Mar Ecol Prog Ser* 54:249–256
- ✦ Diaz RJ, Rosenberg R (2008) Spreading dead zones and consequences for marine ecosystems. *Science* 321:926–929
- ✦ Egger M, Kraal P, Jilbert T, Sulu-Gambari F, Sapart CJ, Röckmann T, Slomp CP (2016) Anaerobic oxidation of methane alters sediment records of sulfur, iron and phosphorus in the Black Sea. *Biogeosciences* 13:5333–5355
- Fahey TJ, Knapp AK (2007) *Principles and standards for measuring primary production*. Oxford University Press, Oxford
- Falkowski PG, Raven JA (1997) *Aquatic photosynthesis*. Blackwell Science, Malden, MA
- Fisheries Bureau of Ministry of Agriculture of the People's Republic of China (2015) *China fishery statistical year-*

- book. China Agriculture Press, Beijing (in Chinese)
- Fisheries Bureau of Ministry of Agriculture of the People's Republic of China (2019) China fishery statistical yearbook. China Agriculture Press, Beijing (in Chinese)
- Grasshoff K, Kremling K, Ehrhardt M (eds) (1999) Methods of seawater analysis, 3<sup>rd</sup> edn. Verlag Chemie, Weinheim
- ✦ He BY, Dai MH, Zhai WD, Guo XH, Wang LF (2014) Hypoxia in the upper reaches of the Pearl River Estuary and its maintenance mechanisms: a synthesis based on multiple year observations during 2000–2008. *Mar Chem* 167:13–24
- ✦ He H, Zhen Y, Mi TZ, Zhang Y, Fu LL, Yu ZG (2015) Distribution of aerobic ammonia-oxidizing microorganisms in sediments from adjacent waters of Rushan Bay. *Environ Sci* 36:4068–4073 (in Chinese)
- ✦ Karim MR, Sekine M, Ukita M (2002) Simulation of eutrophication and associated occurrence of hypoxic and anoxic condition in a coastal bay in Japan. *Mar Pollut Bull* 45: 280–285
- ✦ Kellogg ML, Cornwell JC, Owens MS, Paynter KT (2013) Denitrification and nutrient assimilation on a restored oyster reef. *Mar Ecol Prog Ser* 480:1–19
- ✦ Li DJ, Zhang J, Huang DJ, Wu Y, Liang J (2002) Oxygen depletion off the Changjiang (Yangtze River) Estuary. *Sci China Ser D Earth Sci* 45:1137–1146
- ✦ Li HM, Zhang CS, Han XR, Shi XY (2015) Changes in concentrations of oxygen, dissolved nitrogen, phosphate, and silicate in the southern Yellow Sea, 1980–2012: sources and seaward gradients. *Estuar Coast Shelf Sci* 163:44–55
- ✦ Lin C, Ning X, Su J, Lin Y, Xu B (2005) Environmental changes and the responses of the ecosystems of the Yellow Sea during 1976–2000. *J Mar Syst* 55:223–234
- Lindahl O (2011) Mussel farming as a tool for re-eutrophication of coastal waters: experiences from Sweden. In: Shumway SE (ed) Shellfish aquaculture and the environment. John Wiley and Sons, Hoboken, NJ, p 217–237
- Liu J, Zang JY, Ran XB, Wei QS and others (2012) Characteristics of different forms of nitrogen and phosphorus and organic carbon in the sediments of low-oxygen zones in adjacent Rushan Bay. *Mar Sci* 36:70–78 (in Chinese)
- ✦ Liu J, Zang JY, Zhao CY, Yu Z, Xu B, Li J, Ran X (2016) Phosphorus speciation, transformation, and preservation in the coastal area of Rushan Bay. *Sci Total Environ* 565: 258–270
- ✦ Liu J, Krom MD, Ran XB, Zang JY, Liu JH, Yao QZ, Yu ZG (2020) Sedimentary phosphorus cycling and budget in the seasonally hypoxic coastal area of Changjiang Estuary. *Sci Total Environ* 713:136389
- Long MH, Rheuban JE, McCorkle DC, Burdige DJ, Zimmerman RC (2019) Closing the oxygen mass balance in shallow coastal ecosystems. *Limnol Oceanogr* 9999:1–15
- Ma SS, Zhao J, Zhou SL, Yu HT, Sun KY (1996) Water chemistry environment in Rushan Bay. *Mar Fish Res* 17:63–70 (in Chinese)
- ✦ Middelburg JJ, Levin LA (2009) Coastal hypoxia and sediment biogeochemistry. *Biogeosciences* 6:1273–1293
- National Marine Environmental Monitoring Center (2007) The specification for marine monitoring, Part 4. Seawater analysis. Standards Press of China, Beijing (in Chinese)
- ✦ Paerl HW, Valdes LM, Peierls BL, Adolf JE, Harding L Jr (2006) Anthropogenic and climatic influences on the eutrophication of large estuarine ecosystems. *Limnol Oceanogr* 51:448–462
- Ran XB, Zang JY, Wei QS, Liu W, Guo JS (2011) Characteristics of dissolved oxygen and its influencing factors in the Rushan Bay mouth and its adjacent waters. *Acta Oceanol Sin* 33:173–180 (in Chinese)
- ✦ Riedel GF, Sanders JG, Osman RW (1999) Biogeochemical control on the flux of trace elements from estuarine sediments: effects of seasonal and short term hypoxia. *Mar Environ Res* 47:349–372
- Shandong Provincial Bureau of Statistics (1990–2008) Shandong Rural Statistical Yearbook 1990–2008. China Statistics Press, Beijing (in Chinese)
- Shandong Provincial Department of Oceans and Fisheries (2003–2015) Shandong Fishery Statistical Yearbook 2003–2015. Shandong Provincial Department of Oceans and Fisheries Press, Jinan (in Chinese)
- Shumway SE, Davis C, Downey R, Kraeuter J, Parson J, Rheault R, Wikfors G (2003) Shellfish aquaculture in praise of sustainable economies and environments. *World Aquac* 34:8–10
- ✦ Skjelvan I, Falck E, Anderson LG, Rey F (2001) Oxygen fluxes in the Norwegian Atlantic current. *Mar Chem* 73: 291–303
- ✦ Song G, Liu S, Zhu Z, Zhai W, Zhu C, Zhang J (2016) Sediment oxygen consumption and benthic organic carbon mineralization on the continental shelves of the East China Sea and the Yellow Sea. *Deep-Sea Res II* 124: 53–63
- Sun BN, Dai DJ, Lian Z (2014) The numerical experiment and analysis of pollutant dispersion model in Rushan Bay. In: Wu YC, Yan K, Sun BJ (eds). Proceedings of the 13th National Congress on Hydrodynamics and 26th National Conference on Hydrodynamics. China Ocean Press, Beijing p 601–608 (in Chinese)
- The People's Government of Rushan (1985–2015) Rushan Yearbook. Fangzhi Press, Beijing (in Chinese)
- ✦ Vaquer-Sunyer R, Duarte CM (2008) Thresholds of hypoxia for marine biodiversity. *Proc Natl Acad Sci USA* 105: 15452–15457
- ✦ Wang B, Chen JF, Jin HY, Li HL, Huang DJ, Cai WJ (2017) Diatom bloom-derived bottom water hypoxia off the Changjiang estuary, with and without typhoon influence. *Limnol Oceanogr* 62:1552–1569
- ✦ Wang BD (2009) Hydromorphological mechanisms leading to hypoxia off the Changjiang Estuary. *Mar Environ Res* 67:53–58
- Wang BD, Liu F, Wang GY (1999) Horizontal distributions and seasonal variations of dissolved oxygen in the southern Huanghai Sea. *Acta Oceanol Sin* 21:47–53 (in Chinese)
- ✦ Wang H, Dai MH, Liu JW, Kao SJ, Liu KT, Lee TY (2016) Eutrophication-driven hypoxia in the East China Sea off the Changjiang Estuary. *Environ Sci Technol* 50:2255–2263
- ✦ Wang J, Beusen AHW, Liu X, Bouwman AF (2020) Aquaculture production is a large, spatially concentrated source of nutrients in Chinese freshwater and coastal seas. *Environ Sci Technol* 54:1464–1474
- ✦ Wang ZX, Wei QS, Liu J, Ran XB (2012) Canonical correspondence analysis on macrobenthos community in summer and its environment in the offshore water of Rushan Bay. *Chin J Appl Environ Biol* 18:599–604 (in Chinese)
- ✦ Wanninkhof R (1992) Relationship between wind speed and gas exchange over the ocean. *J Geophys Res Oceans* 97: 7373–7382
- Wei P, Huang LM, Feng JH, Jiang S, Li L, Liu SH, Huang YF (2009) Distribution characteristics of COD and DO and

- its influencing factors in the Guangzhou sea zone of the Pearl River Estuary. *Ecol Environ Sci* 18:1631–1637 (in Chinese)
- Weihai Municipal Bureau of Statistics (1990–2015) Weihai statistical yearbook 1990–2015. [www.rushan.gov.cn](http://www.rushan.gov.cn) (accessed 6 Jan 2016) (in Chinese)
- Weiss RF (1970) The solubility of nitrogen, oxygen and argon in water and seawater. *Deep-Sea Res* 17:721–735
- Xin FY, Ma SS, Yi C, Chen BJ, Chen JF, Zhou SL (1997) Distribution of chlorophyll-*a* content and estimation of the primary productivity in Rushan Bay from June to September. *Mar Fish Res* 18:32–38 (in Chinese)
- Xin FY, Chen BJ, Qu KM, Song JZ, Li QF, Ma SS (2004) The distributions of COD, nitrogen and phosphorus nutrients and nutrient status in Rushan Bay. *Mar Fish Res* 25: 52–56 (in Chinese)
- Yantai Municipal Bureau of Statistics (1985–2015) Statistical yearbook of Yantai 1985–2015. <http://tjj.yantai.gov.cn> (accessed 6 Jan 2016) (in Chinese)
- Zang JY, Zhao CY, Liu J, Xie LP, Wang YB, Zhang AJ, Ran XB (2017) Characteristics and benthic processes of organic carbon in the adjacent area of Rushan Bay. *Zhongguo Huanjing Kexue* 37:1089–1102 (in Chinese)
- ✦ Zhai WD, Zhao HD, Zheng N, Xu Y (2012) Coastal acidification in summer bottom oxygen-depleted waters in north-western-northern Bohai Sea from June to August in 2011. *Chin Sci Bull* 57:1062–1068
- ✦ Zhang J, Gilbert D, Gooday AJ, Levin L and others (2010) Natural and human-induced hypoxia and consequences for coastal areas: synthesis and future development. *Biogeosciences* 7:1443–1467
- Zhang JP, Huang XP, Jiang ZJ, Huang DJ (2009) Seasonal variations of eutrophication and the relationship with environmental factors in the Zhujiang Estuary in 2006–2007. *Acta Oceanol Sin* 31:113–120 (in Chinese)
- Zhang X, Zhu M, Chen S, Grant J, Martin JL (2006) Study on sediment oxygen consumption rate in the Sanggou Bay and Jiaozhou Bay. *Adv Mar Sci* 24:91–96 (in Chinese)
- Zu TT, Bao XW, Xie J, Wu DX (2005) Distribution and variation trends of the environmental factors in the central section of the Bohai Sea. *J Ocean Univ Qingdao* 35: 889–894 (in Chinese)

*Editorial responsibility: Erik Kristensen, Odense, Denmark*

*Submitted: April 15, 2020; Accepted: July 23, 2020  
Proofs received from author(s): September 7, 2020*